

# Continuous-wave coherent ultraviolet source at 326 nm based on frequency tripling of fiber amplifiers

Jae-Ihn Kim\* and Dieter Meschede

*Institut für Angewandte Physik, Universität Bonn, Wegelerstraße 8, 53115 Bonn, Germany*

[\\*kim@iap.uni-bonn.de](mailto:kim@iap.uni-bonn.de)

**Abstract:** We have demonstrated a tunable single frequency source of continuous-wave (CW) coherent ultraviolet (UV) radiation at  $\lambda_{3\omega} = 326$  nm. Laser light of a tunable diode laser at  $\lambda_{\omega} = 977$  nm was split and injected into two independent fiber amplifiers yielding 1 W and 0.4 W, respectively. The 1 W branch was resonantly frequency doubled, resulting in 120 mW of useful power at  $\lambda_{2\omega} = 488$  nm. The third harmonic was generated by summation of the second branch of  $\lambda_{\omega}$  and  $\lambda_{2\omega}$  which were enhanced by a doubly resonant cavity. This light source has TEM<sub>00</sub> character and can be continuously tuned over more than 18 GHz. It is of interest for efficient laser cooling of In and potentially other applications.

© 2008 Optical Society of America

**OCIS codes:** (060.2320) Fiber optics amplifiers and oscillators; (140.3610) Lasers, ultraviolet; (190.2620) Harmonic generation and mixing; (140.3600) Lasers, tunable

---

## References and links

1. D. Meschede and H. Metcalf, "Atomic nanofabrication: atomic deposition and lithography by laser and magnetic forces," *J. Phys. D* **36**, R17–38 (2003).
2. E. S. Polzik and H. J. Kimble, "Frequency doubling with KNbO<sub>3</sub> in an external cavity," *Opt. Lett.* **16**, 1400–1402 (1991).
3. S. Bourzeix, M. D. Plimmer, F. Nez, L. Julien, and F. Biraben, "Efficient frequency doubling of a continuous wavetitanium:sapphire laser in an external enhancement cavity," *Opt. Commun.* **99**, 89–94 (1993).
4. S. Sayama and M. Ohtsu, "Tunable UV CW generation by frequency tripling of a Ti:sapphire laser," *Opt. Commun.* **137**, 295–298 (1997).
5. J. Mes, E. J. van Duijin, R. Zinkstok, S. Witte, and W. Hogervorst, "Third-harmonic generation of a continuous-wave Ti:Sapphire laser in external resonant cavities," *Appl. Phys. Lett.* **82**, 4423–4425 (2003).
6. H. Kumagai, and K. Midorikawa, T. Iwane, and M. Obara, "Efficient sum-frequency generation of continuous-wave single-frequency coherent light at 252 nm with dual wavelength enhancement," *Opt. Lett.* **28**, 1969–1971 (2003).
7. A. Friedenauer, F. Markert, H. Schmitz, L. Petersen, S. Kahra, M. Herrmann, Th. Udem, and T. W. Hänsch, and T. Schätz, "High power all solid state laser system near 280 nm," *Appl. Phys. B* **84**, 371–373 (2006).
8. P. Herskind, J. Lindballe, C. Clausen, J. L. Sorensen, and M. Drewsen, "Second-harmonic generation of light at 544 and 272 nm from an ytterbium-doped distributed-feedback fiber laser," *Opt. Lett.* **32**, 268–270 (2007).
9. T. Südmeyer, Y. Imai, H. Masuda, N. Eguchi, M. Saito, and S. Kubota, "Efficient 2<sup>nd</sup> and 4<sup>th</sup> harmonic generation of a single-frequency, continuous-wave fiber amplifier," *Opt. Express* **16**, 1546–1551 (2008).
10. J. Nilsson, J. D. Minelly, R. Paschotta, A. C. Tropper, and D. C. Hanna, "Ring-doped cladding-pumped single-mode three-level fiber laser," *Opt. Lett.* **23**, 355–357 (1997).
11. S. Jetschke, S. Unger, U. Röpke, and J. Kirchhof, "Photodarkening in Yb doped fibers: experimental evidence of equilibrium state depending on the pump power," *Opt. Express* **15**, 14838–14843 (2007).
12. R. Paschotta, J. Nilsson, A. C. Tropper, and D. C. Hanna, "Ytterbium-doped fiber amplifiers," *IEEE J. Quantum Electron.* **33**, 1049–1056 (1997).
13. G. D. Boyd and D. A. Kleinman, "Parametric interaction of focused Gaussian light beams," *J. Appl. Phys.* **39**, 3597–3639 (1968).

14. T. W. Hänsch and B. Couillaud, "Laser frequency stabilization by polarization spectroscopy of a reflecting reference cavity," *Opt. Commun.* **35**, 441–444 (1980).
  15. J. Hald, "Second harmonic generation in an external ring cavity with a Brewster-cut nonlinear crystal: theoretical considerations," *Opt. Commun.* **197**, 169–173 (2001).
  16. Y. Kaneda, and S. Kubota, "Theoretical treatment, simulation, and experiments of doubly resonant sum-frequency mixing in an external resonator," *Appl. Opt.* **36**, 7766–7775 (1997).
- 

## 1. Introduction

Laser cooling is a well established technique for controlling the motion of neutral atoms. While it is in widespread use for the generation of e.g. cold alkali gases for fundamental research, it is also of interest for applications, e.g. atomic nanofabrication (ANF) [1]. Technologically relevant materials such as indium and other elements of the third group of the periodic table and others frequently offer only short wavelength UV optical transitions suitable for laser cooling, i.e. exhibiting a closed strong dipole transition allowing a high rate of absorption-emission cycles. The applicability of these methods thus depends very much on the availability of robust and not too expensive sources of coherent, intense light at short wavelengths. In our laboratory we are experimenting with a laser cooled In atomic beam. With such a beam the methods of ANF could for example allow the generation of a fully 3D structured (In,Al)As crystal with periodically modulated In concentration.

For laser manipulation of In atoms the  $5P_{3/2}$ - $5D_{5/2}$  states offer an excellent cycling transition for UV light at 325.6 nm. While at present no direct single frequency laser exists not to speak of tunable laser light sources at this wavelength, it can be generated straightforwardly by frequency doubling a 651 nm dye laser. For applications, however, robust solid state laser sources are much preferred. The recent and very rapid evolution of fiber lasers and fiber amplifiers suggests their application as coherent UV light sources by upconversion with appropriate nonlinear processes. Fiber lasers and amplifiers are compact and economic, and their light offers excellent diffraction limited beam quality. They are thus ideally suited to replace Ti:sapphire lasers for efficient UV generation [2, 3, 4, 5, 6] as has been shown for second and fourth harmonic generation in [7, 8, 9] already. The adoption of upconversion schemes from infrared to UV frequencies with fiber devices renders applications possible which up to now were impaired by the complex and costly operation of Ti:sapphire system, e. g. atom lithography with 3rd group elements.

In this paper we describe a fiber-based CW coherent UV light source which is based on generating the third harmonic of 977 nm light. The upconverted light at 326 nm is suitable for laser cooling of In atoms and other applications. A seed laser at the fundamental wavelength  $\lambda_\omega$  is amplified by two independent fiber amplifiers. Then, one of the infra-red light beams at  $\lambda_\omega$  is frequency doubled in an external cavity (EC). Subsequently, the  $\lambda_\omega$  light from the second fiber amplifier and the second-harmonic (SH) light at  $\lambda_{2\omega}$  are coupled into a doubly resonant cavity in order to generate third-harmonic light at  $\lambda_{3\omega}$ .

## 2. Two fiber amplifiers seeded by a single ECDL

The schematic of our experimental setup is shown in Fig. 1. As a seed source we employ a home-built external cavity diode laser (ECDL) emitting  $\lambda_\omega$  at 977 nm. Two 60 dB optical isolators protect the ECDL from backreflections. A 920 nm, 40 W multi-mode diode laser module (Fianium PUMA-920-40) serves as a pump source. As a gain medium for the amplification of the seed power, an Yb-doped double clad fiber (YDCF) is selected. Because of a large absorption peak of Yb ions at  $\sim 977$  nm, a special fiber (Crystal Fibre DC-27-6-Yb) with a small inner cladding is required in order to reduce the threshold pump power and suppress unwanted emission at  $\sim 1040$  nm [10]. The diameters of the core and inner cladding of the fiber used in this

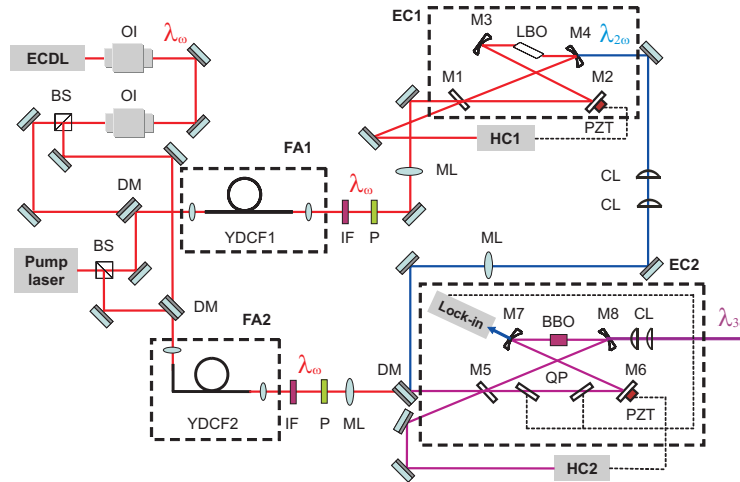


Fig. 1. Experimental setup. Our system uses a diode laser system (ECDL), two fiber amplifiers (FA) and two external cavities (EC) for upconversion,  $\lambda_{\omega} \rightarrow \{\lambda_{\omega}, \lambda_{2\omega}\} \rightarrow \lambda_{3\omega}$ . ECDL, external cavity diode laser; EC, external cavity; YDCF, Yb-doped double clad fiber; HC, Hänsch-Couillaud method; OI, optical isolator; DM, dichroic mirror; M, mirror; CL, cylindrical lens; ML, mode-matching lens; IF, interference filter; PZT, piezo-electric transducer; BS, beam splitter; P, polarizer; QP, quartz plate.

experiment are 6 and 27  $\mu\text{m}$ , respectively. The numerical aperture (NA) of the inner cladding is 0.55. The fibers are angle cleaved ( $\sim 8^\circ$ ) in order to suppress back-reflection induced lasing. The measured pump absorption is 1.1 dB/m. Two independent fiber amplifiers are used rather than just splitting the output beam from one amplifier in order to obtain efficient operation and to escape the photo darkening effect caused primarily by a high population inversion which is required in 3 level Yb-doped fiber light sources at  $\sim 977$  nm [11]. We split the seed and pump beams into two beams each and form two seed-pump beam pairs by combining them with a dichroic mirror. The pairs are then coupled to the YDCFs by a 3.1 mm focal length and 0.68 NA collimating lens. At each output port of the FAs, the pump light is eliminated by an interference filter.

Figure 2 shows the experimental and theoretical output power from both FAs as a function of the launched pump power. The lengths of the first (FA1, YDCF1) and the second (FA2, YDCF2) fibers are 1.2 m and 0.8 m, respectively. With 14 W pump power launched into each FA, we obtain 1.26 W (0.63 W) at  $\lambda_{\omega}$  from FA1 (FA2) using 20 mW (15 mW) seed power. Solid lines are the calculated output powers based on a rate equation model [12], and experiment and theory are in good agreement. The corresponding gains are 18 dB for FA1 and 16 dB for FA2. The amplified spontaneous emission (ASE) is suppressed by more than 33 dB below the carrier as measured with an optical spectrum analyzer. Although the YDCF is non-polarization preserving, we have small polarization fluctuations only. We further improve the polarization stability by introducing a polarizer at the expense of slow amplitude fluctuations at the few percent level.

### 3. Second harmonic generation in an external cavity

The output of FA1 is frequency-doubled in an external cavity [2, 3] as shown in the upper right corner of Fig. 1. We employ a Brewster-cut type-I phase-matched  $\text{LiB}_3\text{O}_5$  (LBO) crystal with length 10 mm. The reflectivity of the input mirror M1 for  $\lambda_{\omega}$  is 98.3 %, and the output mirror M4

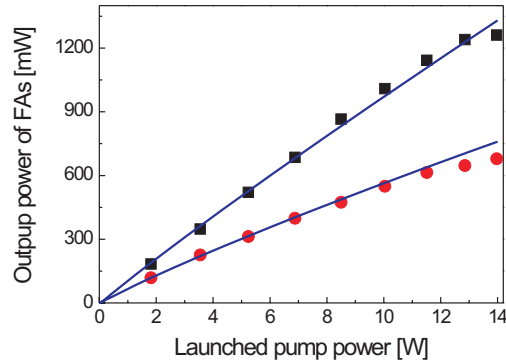


Fig. 2. Experimental output powers of FA1 (rectangles) and FA2 (circles) at 977 nm as a function of the launched pump power at  $\sim 920$  nm. The solid lines show the theoretical output powers. Suppression of ASE is more than 33 dB below the carriers as measured with an optical spectrum analyzer.

is dichromatically coated to provide high reflectivity for  $\lambda_{\omega}$  and 95 % transmission at  $\lambda_{2\omega}$ . The radii of curvature of M3 and M4 were chosen to be -50 mm, and the distance between the two curved mirrors is optimized to maximize the Boyd-Kleinman factor [13]. A small mirror M2 is mounted on a piezoelectric transducer (PZT) to lock the cavity length to  $\lambda_{\omega}$  by the Hänsch-Couillaud method [14]. The angle of incidence of M3 and M4 is chosen to compensate the astigmatism caused by the crystal Brewster surfaces [15]. The waists of the eigen mode at the center of the LBO crystal are calculated to be  $36 \mu\text{m}$  in the tangential and  $24 \mu\text{m}$  in the sagittal plane. The blue radiaton at  $\lambda_{2\omega}$  emitted from the cavity is mode-matched to EC2 by a spherical and two cylindrical lenses.

Figure 3 shows the experimental and theoretical SH power at  $\lambda_{2\omega}$  as a function of the incident fundamental power. The maximum SH power measured behind the mirror M4 is 120 mW at 915 mW fundamental power. The circulating power of 87 W is estimated by measuring the infrared power leaking from M3. A single-pass conversion efficiency of  $2 \times 10^{-5} \text{ W}^{-1}$  is deduced corresponding to 46 % of the calculated value. The difference between the measured and calculated single-pass conversion efficiency may be attributed to the deviation of the effective nonlinear coefficient from the specified value used for the calculation. Also insufficient knowledge about focusing parameters may play a role. The linear loss of 0.44 % per round trip in the cavity is inferred from a measurement of the reflected fundamental power yielding an estimated mode-matching efficiency of 74 % [6]. The overall conversion efficiency is 13 %, and internal conversion efficiency with respect to the incoupled fundamental power is 27 %. The solid line in Fig. 3 is a theoretical curve based on the measured parameters. The measured and the theoretical second harmonic power are in good agreement.

#### 4. Third harmonic generation in a doubly resonant cavity

Third harmonic generation is based on the frequency upconversion of  $\lambda_{2\omega}$  light from the EC1 and another  $\lambda_{\omega}$  beam from FA2 [4, 5]. The blue light beam at  $\lambda_{2\omega}$  from the first enhancement cavity (EC1) and the second infrared light beam at  $\lambda_{\omega}$  from FA2 are combined by a dichroic mirror and then coupled to the second bow-tie shaped cavity through mode matching lenses as shown at the bottom right corner of Fig. 1. Here a 10-mm-long type-I phase-matched  $\beta$ -BaB<sub>2</sub>O<sub>4</sub>

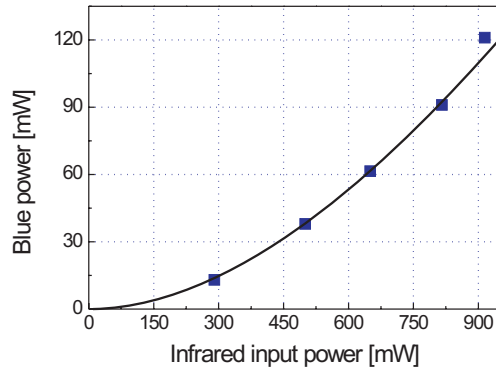


Fig. 3. Experimental (rectangles) and theoretical (solid line) second harmonic power at 488 nm as a function of the input power at 977 nm.

(BBO) crystal was chosen, since it has high transmission at UV wavelengths. Both of the facets of the BBO crystal are antireflection coated for  $\lambda_\omega$ ,  $\lambda_{2\omega}$  and  $\lambda_{3\omega}$  light. The input coupler M5 has 98.5 % reflectivity at  $\lambda_\omega$  and 97 % reflectivity at  $\lambda_{2\omega}$ . A small mirror M6 is mounted on a low-voltage PZT to keep the cavity resonant. The output coupler M8 has high reflectivity for  $\lambda_\omega$ ,  $\lambda_{2\omega}$ , and 87 % transmission for  $\lambda_{3\omega}$ . The radii of curvature of the curved mirrors M7 and M8 are -75 mm. The distance between the mirrors is optimized for maximum conversion efficiency. The angle of incidence of the second cavity is  $12^\circ$ . The waist is calculated to be  $43 \mu\text{m}$  for  $\lambda_\omega$  and  $24 \mu\text{m}$  for  $\lambda_{2\omega}$  light.

To maintain the second cavity simultaneously resonant with the  $\lambda_\omega$  and  $\lambda_{2\omega}$  wavelengths, two steps are used [5]. The length of EC2 is locked to the  $\lambda_\omega$  wavelength using the Hänsch-Couillaud method [14]. A small optical path length difference (OPD) between  $\lambda_\omega$  and  $\lambda_{2\omega}$  caused by dispersion in the cavity is compensated by slightly rotating two quartz plates mounted at Brewster's angle. The thickness of each plate is 2 mm and tuning the angle by  $\pm 0.2^\circ$  can cover 250 nm OPD corresponding to  $\sim$  the half wavelength of  $\lambda_{2\omega}$ . The quartz plates are mounted on counter rotating galvo motors and dithered at 270 Hz. Phase sensitive detection of the blue light at  $\lambda_{2\omega}$  leaking from M7 allows us to derive an error signal for compensating cavity dispersion, so that EC2 is resonant for the blue wavelength  $\lambda_{2\omega}$ , too.

The experimental values of third harmonic power at  $\lambda_{3\omega}$  as a function of the input power at  $\lambda_\omega$  are shown in Fig. 4. The maximum third harmonic power at  $\lambda_{3\omega}$  measured behind the output coupler M8 is 12 mW for 405 mW at  $\lambda_\omega$  and 120 mW at  $\lambda_{2\omega}$ , respectively. The measured circulating powers are 26 W for  $\lambda_\omega$  and 2.4 W for  $\lambda_{2\omega}$ . The estimated single-pass conversion efficiency is  $2.2 \times 10^{-4} \text{ W}^{-1}$ , which is 88 % of the calculated value. By measuring the rejected power of the blue and infrared beam from EC2, the linear losses are estimated to be 1.23 % for  $\lambda_\omega$  and 2 % for  $\lambda_{2\omega}$ . The mode-matching efficiencies are calculated to be 80 % for  $\lambda_\omega$  and 49 % for  $\lambda_{2\omega}$  beam. The overall conversion efficiency is 2.3 %, and the internal efficiency with respect to the coupled fundamental waves is 3.6 %. The result of a theoretical calculation [16] of the UV power based on the measured parameters is shown in the solid line in Fig. 4, and the theory agrees well with the experimental result. The mode-hop free tuning range of UV light is more than 18 GHz.

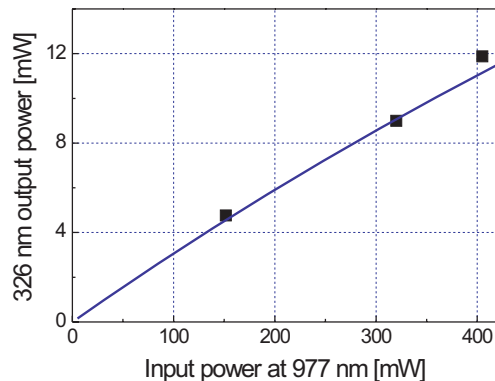


Fig. 4. Experimental (rectangles) and theoretical (solid line) third harmonic power at 325 nm as a function of the input power at 977 nm. Blue light power at 488 nm is fixed at 120 mW.

## 5. Conclusion

In summary, we have developed a tunable single-mode UV source at  $\lambda_{3\omega}$ . Two FAs using a single seed laser were built to generate 1 W (FA1) and 0.4 W (FA2) fundamental power for nonlinear frequency conversion. The output of FA1 was frequency doubled in a cavity to generate 120 mW blue light at  $\lambda_{2\omega}$ . To generate UV light at  $\lambda_{3\omega}$  through third harmonic generation, the output of FA2 and the second harmonic light beam at  $\lambda_{2\omega}$  were coupled into the second cavity which was doubly resonant with both  $\lambda_{\omega}$  and  $\lambda_{2\omega}$  wavelengths. We have obtained 12 mW UV light at  $\lambda_{3\omega}$  and tuned the UV laser frequency continuously more than 18 GHz.

Realistic improvements of our system include a longer fiber for FA2 (1 W instead of 0.4 W) and a reduction of intracavity loss in EC1 (400 mW instead of 120 mW at  $\lambda_{2\omega}$ ). Then we should approach 100 mW output power at  $\lambda_{3\omega} = 326$  nm. Already with the current setup a UV light source suitable for laser cooling of indium with the  $5P_{3/2}-5D_{5/2}$  closed transition is available.

## Acknowledgments

This work was supported by the NANOCOLD project of the European Commission. We thank P. Georges for fruitful discussions on high power fundamental sources at 977 nm.